Ab initio investigations of the charge transport properties of endohedral M@C_{20} (M = Na and K) metallofullerenes*

An Yi-Peng (安义鹏), Yang Chuan-Lu(杨传路)†, Wang Mei-Shan(王美山), Ma Xiao-Guang(马晓光), and Wang De-Hua(王德华)

School of Physics, Ludong University, Yantai 264025, *China*

(Received 1 March 2010; revised manuscript received 6 March 2010)

Using density functional theory and quantum transport calculations based on nonequilibum Green's function formalism, we investigate the charge transport properties of endohedral M@C_{20}(M = Na and K) metallofullerenes. Our results show that the conductance of C_{20} fullerene can be obviously improved by insertion of alkali atom at its centre. Both linear and nonlinear sections are found on the I–V curves of the Au-M@C_{20}-Au two-probe systems. The novel negative differential resistance behaviour is also observed in Na@C_{20} molecule but not in K@C_{20}.

Keywords: M@C_{20} metallofullerenes, electronic transport, density functional theory, nonequilibum Green's function

PACC: 3450D, 3640, 7280R

1. Introduction

Electronic transport calculations through molecular and nanoelectronic devices are currently attracting much attention in nanoscience and nanotechnology[1−9] because of their novel physical properties and potential applications in electronic devices, such as single-electron characteristic,[10] negative differential resistance (NDR) behaviour,[11,12] electrostatic current switching,[13] etc. Various forms of carbon nano-structures, namely, buckyball,[14] carbon nanotube,[15] have aroused a great deal of interest due to their novel fundamental properties and possible applications in electronics. More importantly, with the progresses in microfabrications and self-assembly techniques,[16] carbon-based nanostructures have emerged as one of the most promising materials for nonsilicon electronics.

Fullerenes and endohedral metallofullerences[17−19] have attracted wide interest because of their functional characteristics and potential applications in the fields of nanomaterials and biomedical science. The C_{20} molecule, consisting solely of pentagons, is the smallest unconventional fullerene which breaks the 'isolated pentagon rule'. This fullerene is expected to have larger vibronic coupling than C_{60}, and its solid form could be a good candidate for a superconductor.[20] So, it is significant to study the structural, electronic, and transport properties of C_{20} and its endohedral metallofullerenes, which are all expected to produce novel functional molecular devices.

In the previous work,[21] we have investigated the transport properties of C_{20} fullerene and its endohedral metallofullerene Li@C_{20}. It is found that the Li atom significantly varies the transport properties of C_{20} fullerene and makes it show novel NDR behaivour, which implies that Li@C_{20} molecule could be used as a candidate of the NDR molecular devices. To know more about the effects of other alkali metal atoms on the transport properties of C_{20}, we extend our investigations to the M@C_{20} (M = Na and K) molecules in this paper.

2. Methodology

The charge transport properties of the endohedral M@C_{20} (M = Na and K) metallofullerenes are calculated with the Atomistix ToolKit (ATK) software package,[22,23] which combines density functional theory (DFT) and non-equilibrium Green's function (NEGF)[23−25] method. This method has been used by several groups in a variety of applications and is well documented.[24−28] In brief, the charge density is computed within the Keldysh NEGF theory, taking into account the open system boundary conditions through an iterative procedure. Once the Kohn–

*Project supported by the National Natural Science Foundation of China (Grant Nos. 10674114 and 10974078).

†Corresponding author. E-mail: yangchuanlu@263.net Present address: Surface Physics Laboratory (National Key Laboratory), Fudan University, Shanghai 200433, China

© 2010 Chinese Physical Society and IOP Publishing Ltd

Sham effective potential has been self-consistently converged, the transport properties of the molecule are obtained.

Our calculations use a two-probe model as shown in Fig. 1. Each molecule is rigidly attached to Au (111) surface. In practical theoretical simulation, such a two-probe system is divided into three parts: the left electrode, the right electrode, and the central scattering region. The scattering region actually includes a portion of the semi-infinite electrodes. In order to compare the effect by doping different alkali metal atoms into C_{20}, we have used the same molecule-electrode contact configuration like that of Li@C_{20}.[21] The distance between the molecule and electrodes is also fixed at 2.185 Å (1 Å = 0.1 nm). To save computational efforts and improve calculating precision and reliability, valence electrons are expanded in single zeta plus polarisation (SZP) basis sets for metal electrode (Au atom) and double zeta plus polarisation (DZP) basis for other atoms. The norm-conserving Troullier–Martins pseudopotentials[29] are used to describe the core electrons for all atoms. The exchange–correlation potential is described by the Perdew–Burke–Ernzerhof (PBE) parametrisation of generalised gradient approximation (GGA) function.[30] The electrode calculations are performed under periodical boundary conditions, with the unit cell being three layers along the transport direction, and the Brillouin zone has been sampled with 3×3×100 points within the Monkhorst–Pack k-point sampling scheme in the case of our three-dimensional two-probe systems. The self-consistent calculations are performed with a mixing rate set to 0.01 and the convergent criterion for total energy is 10^{-5} eV. The electrostatic potentials are determined on a real-space grid with a mesh cutoff energy of 110 Ry to achieve a balance between the calculation efficiency and accuracy.

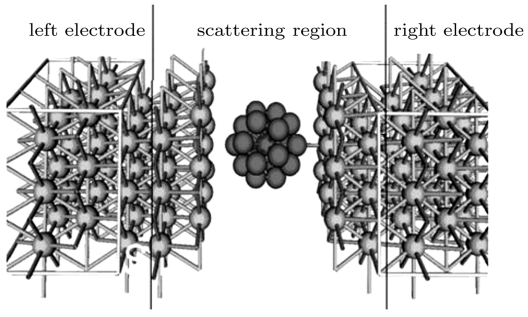


Fig. 1. The geometry of the two-probe systems Au (111)-M@C_{20}-Au (111). Each molecule together with two surface gold layers on the left and right electrodes is included in the self-consistent calculation.

The current through the atomic scale system is calculated from Landauer–Büttiker formula[31]

$$I = \frac{2e}{h}\int T(E,V_{\rm b})[f_{\rm L}(E-\mu_{\rm L}) - f_{\rm R}(E-\mu_{\rm R})]\,{\rm d}E, \quad (1)$$

where $V_{\rm b}$ is the applied bias voltage, and $\mu_{\rm L}$ and $\mu_{\rm R}$ are the electrochemical potentials of the left and right electrodes, respectively, $\mu_{\rm L}-\mu_{\rm R}=eV_{\rm b}$. The energy region between $\mu_{\rm L}$ and $\mu_{\rm R}$, which contributes to the current integral above, is referred to as the bias window. While $f_{\rm L}$ and $f_{\rm R}$ are the Fermi–Dirac distribution functions of the left and right electrodes, respectively. $T\,(E,V_{\rm b})$ is the transmission coefficient at energy E and bias voltage $V_{\rm b}$. Based on the eigenchannel decomposition of the conductance, the total transmission probability $T\,(E)$ can be decomposed into non-mixing eigenchannels $T_n(E)$,[32] $T(E)=\sum_n T_n(E)$, and can be calculated from the formula as

$$T(E,V_{\rm b}) = {\rm Tr}\left[\Gamma_{\rm L}\,(E)\,G^{\rm R}(E)\Gamma_{\rm R}\,(E)\,G^{\rm A}(E)\right], \quad (2)$$

where $G^{\rm R}(E)$ and $G^{\rm A}(E)$ are the retarded and advanced Green's functions of the central scattering region, and $\Gamma_{\rm L}$ and $\Gamma_{\rm R}$ are the contact broadening functions (or named coupling matrix) associated with the left and right electrodes, respectively. The broadening functions are anti-Hermitian components of the self-energy terms of the contacts, $\Sigma_{\rm L}$ and $\Sigma_{\rm R}$, which depend on the electrode's surface Green's function and the contact-molecule bonding: $\Gamma_{\rm L,R} = {\rm i}\left(\Sigma^{\rm R}_{\rm L,R}-\Sigma^{\rm A}_{\rm L,R}\right)/2$. For the system at equilibrium, the conductance G is evaluated by the transmission coefficients $T(E)$ at the Fermi energy $E_{\rm F}$ of the system $G=G_0T(E_{\rm F})$, where $G_0=2e^2/h$ is the fundamental quantum conductance unit.

3. Results and discussion

The stable structures of Na@C_{20} and K@C_{20} are first obtained using first-principles DFT method as implemented in the DMol^3 software package.[33] The exchange correlation energy is calculated using GGA with the parametrisation of Perdew and Wang (PW91).[34] The energy tolerance in the self-consistent field calculations is set to 10^{-6} Hartree. Optimised geometries are obtained using an energy convergence tolerance of 10^{-5} Hartree with the force on each atom less than 5.0×10^{-4} Hartree/Bohr. The frequency analysis has been performed to validate the energetic stability of all the molecules. The vibrational spectra are calculated in the harmonic approximation using the

finite displacement technique to obtain the force constant matrix. The maximum allowed change in any Cartesian coordinate is set to 0.002 Å in order to obtain more accurate geometries. This method has well been used in the previous work.[35−38] After the geometry optimisation and vibration frequency analysis, the stable structures of Na@C_{20} and K@C_{20} molecules are obtained.

To show the process in which Na or K is inserted into the C_{20} cage, we place the Na or K at different distance from the centre of the cage and calculate the energy curve versus the distance. For the sake of clarity, only the energy curve for K is plotted in Fig. 2. We can find from the figure that the whole inserting process is endothermic. However, there is a barrier at the surface of the C_{20} cage. There is an obvious exothermic process after the K atom getting into the cage. It means that the K atom can spontaneously go to the centre of the C_{20} cage and stay there as long as it approaches and passes through the surface. Therefore the synthesis is not very difficult.

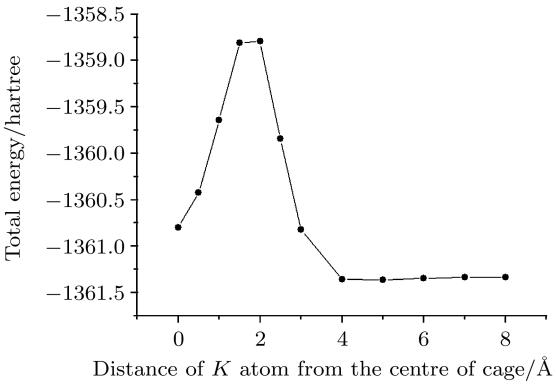


Fig. 2. The energy curve of K inserted into C_{20} Cage.

Based on the method described in Section 2, we first probe the equilibrium transport properties of Na@C_{20} and K@C_{20}, which are symmetrically sandwiched between the three-dimensional Au electrodes. The most important physical quantity in NEGF-DFT calculations for electronic transport through single molecular junctions is the transmission function $T(E)$. Its value at the Fermi level defines the zero-bias conductance, and its integral over the bias-dependent energy window gives the current. Therefore, we first calculate the transmission functions $T(E)$ of both the two-probe systems under zero bias, and show them in Fig. 3. For the sake of clarity, the Fermi level has been shifted to $E_{\rm F} = 0$.

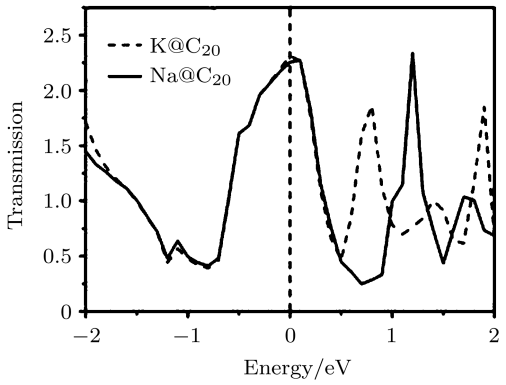


Fig. 3. The zero bias transmission spectra of the two-probe systems Au (111)-M@C_{20}-Au (111). The energy is relative to the Fermi level (vertical line).

In the case of Na@C_{20} molecule, the calculated equilibrium conductance is $2.257G_0$, which is slightly larger than that ($2.198G_0$) of Li@C_{20}[21] and also larger than that ($1.315G_0$) of C_{20}. For K@C_{20} molecule, its equilibrium conductance is about $2.312G_0$, slightly larger than that of both Na@C_{20} and Li@C_{20} molecules. So, the interstitial Na or K atom can obviously improve the conductance of C_{20}.

This enhancement of conductance by inserting Na or K atom into C_{20} can be understood by the effective method in which the self-consistent Hamiltonian of the molecular junction is projected onto the molecule and the molecular projected self-consistent Hamiltonian (MPSH) matrix is diagonalised. Related MPSH states are the eigenstates of the molecular system placed in a two-probe environment. As we know, the properties of the highest occupied molecular orbital (HOMO) and lowest unoccupied molecular orbital (LUMO) are often especially important for the electronic properties, because electron transitions typically take place between these two orbitals. The MPSH eigenstates of the HOMO and LUMO of the two-probe systems are presented in Fig. 4. The molecular orbital occupation states of Au-C_{20}-Au[21] are also included as a reference. The charge distributions of HOMOs (Figs. 4(a), 4(c), and 4(e)) of these two-probe systems show similar characteristics, while the LUMOs display differences. In comparison with the LUMO of Au-C_{20}-Au (Fig. 4(e)), more charge distributions and obvious bonding between two carbon atoms are observed on the LUMOs of Na@C_{20} and K@C_{20}. This fact makes the electron easier to tunnel through C_{20}. So, the conductibility of C_{20} is improved by the interstitial Na or K atom.

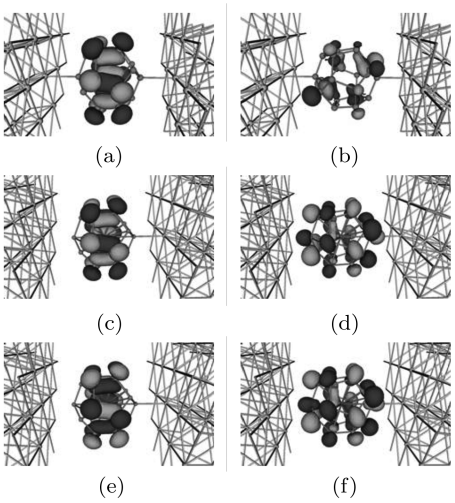


Fig. 4. Molecular orbital occupation states of the two-probe systems: (a) HOMO of the MPSH states of Au-C_{20}-Au; (b) LUMO of MPSH states of Au-C_{20}-Au; (c) HOMO of the MPSH states of Au-Na@C_{20}-Au; (d) LUMO of MPSH states of Au-Na@C_{20}-Au; (e) HOMO of the MPSH states of Au-K@C_{20}-Au; (f) LUMO of MPSH states of Au-K@C_{20}-Au.

The zero-bias transmission spectrum is not sufficient to describe the charge transport properties of a molecule. The current–voltage (I–V) curve is a more important property in designing a molecular device. Therefore, it is necessary to investigate the change of the transport properties under the applied bias voltage. Figure 5 shows our calculated I–V curves of both Na@C_{20} and K@C_{20} molecules. The considered bias voltage varies from –2.0 to 2.0 V.

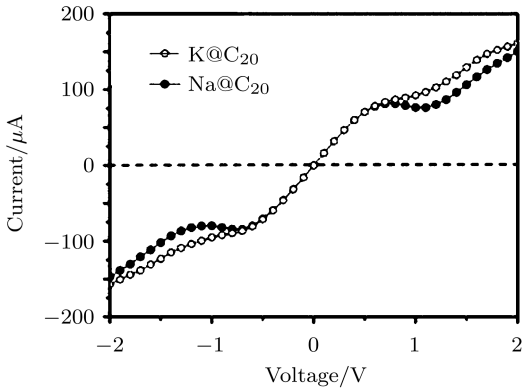


Fig. 5. Current–voltage (I–V) curves of the two-probe systems.

From Fig. 5, it can be seen that their I–V curves show linear and nonlinear characteristics. Under low bias voltages (from –0.7 to 0.7 V), the two I–V curves present linear current–voltage characteristic, and nearly overlap each other. It implies that both Na@C_{20} and K@C_{20} behave like metal in this voltage range. When the bias is beyond 0.7 or −0.7 V, both I–V curves show nonlinear characteristic, but the two molecules display different behaviour. For Na@C_{20}, a maximum on the I–V curve suggests that the molecule has the novel NDR behaviour like Li@C_{20}.[21] As we all know, NDR behaviour is very important in the field of electronic technology. Lots of applications in the area of semiconductor physics, including amplification,[39] digital applications and oscillators,[40] have been found since it was discovered.[11] The NDR behaviour of Na@C_{20} makes it a potential candidate for NDR molecular device. While for K@C_{20}, no NDR phenomenon is observed.

Characteristics of the I–V curves can be well explained by the transmission spectra obtained at different bias voltages, because the current is directly dependent on the transmission coefficient based on the Landauer–Büttiker formula. The calculated transmission spectra $T(E, V_b)$ for different applied bias voltages from –2.0 to 2.0 V (each curve represents a difference of 0.1 V) are presented in Fig. 6. The bias window contributing to the current integral in Eq. (1) is indicated by the two dotted lines in this figure. For Na@C_{20} molecule, as shown in Fig. 6(a), we can see that under low bias (from –0.7 to 0.7 V), the transmission coefficients within bias window hardly change with the increase of bias voltage, which makes the current linearly increase along with the bias increasing. While in the ranges from 0.7 to 1.2 V (or from –0.7 to –1.2 V), the transmission resonances within bias window obviously reduce. As a result, the integration value (current) decreases and NDR phenomenon exhibits. When the bias reaches larger values (beyond 1.2 or –1.2 V), more resonances enter into the bias window and contribute to the current. Therefore, the current continues to increase. For K@C_{20} (Fig. 6(b)), when the bias is beyond 0.7 or –0.7 V, the transmission coefficients within bias window also reduce but the gradient is smaller than that of Na@C_{20} molecule, which results in that the current always increases smoothly. Therefore there is no NDR behaviour for K@C_{20}.

Another characteristic of the I–V curves can also be understood by the properties of the molecular orbital energy levels. As shown in Fig. 7, we depict the HOMO–LUMO gaps (H–Lgs) of both Na@C_{20} and K@C_{20}. Under low bias voltage (from –0.7 to 0.7 V), the H–Lgs of the two molecules are very small, and the electron can easily tunnel through the molecule. So, the current through the molecules will increase

quickly with increasing bias, which corresponds to the linear segment (from –0.7 to 0.7 V) of the I–V curves. When the bias reaches –0.7 or 0.7 V, for Na@C_{20} molecule, the H–Lgs also increase to about 0.7 eV. The transition probability of electron between HOMO and LUMO will increase because of the almost same energy values of H–Lgs and bias. It obviously decreases the tunneling probability of the electron, and makes the current through Na@C_{20} diminish. It is responsible for the NDR behaviour of Na@C_{20}. When the bias is beyond 1.2 or –1.2 V, the electron carrying more energy can easily tunnel through the molecule. So the current will continue to increase under higher bias. However, for K@C_{20} molecule, the H–Lgs do not display the obvious change like that of Na@C_{20}. Therefore, the electron can always tunnel through the molecule and the current always increases with the increase of bias voltage. So no NDR behaviour exhibits for K@C_{20} molecule.

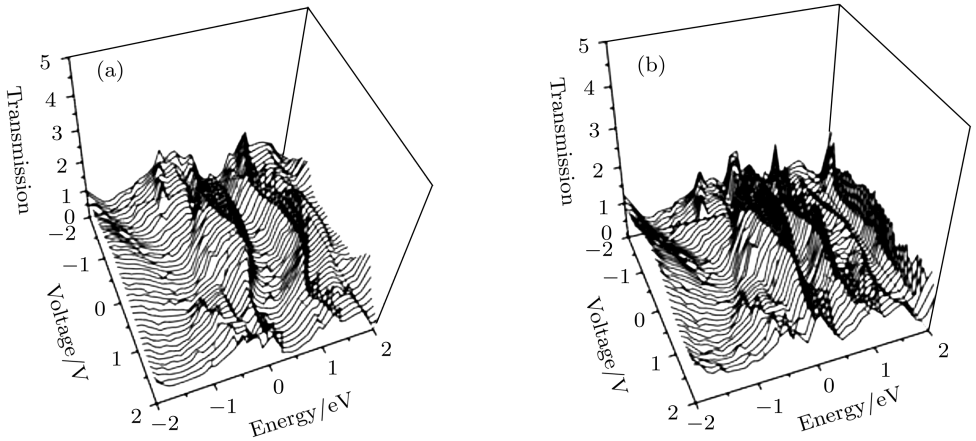


Fig. 6. Transmission spectra $T(E, V_b)$ at different biases: (a) for Na@C_{20} and (b) for K@C_{20}. The two crossing dotted lines indicate the bias window.

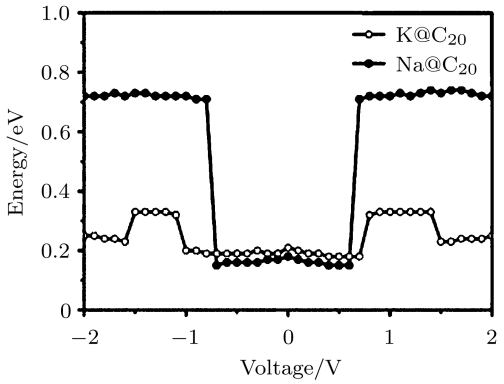


Fig. 7. The HOMO–LUMO gap of both the molecular devices.

We also calculate the conductances of the two molecules under various biases from –2.0 to 2.0 V and the results are shown in Fig. 8. Under low bias voltage, both molecular devices present similar electronic conductivity. Although their I–V curves in Fig. 5 present linear characteristics in the range from –0.7 to 0.7 V, the calculated conductances show a little deviation from the invariable, but the largest error is no more than 13%. When the bias is beyond 0.7 or –0.7 V, K@C_{20} has a larger conductance than Na@C_{20}, which implies that K@C_{20} molecule has better conductibility in this range. However, their conductances tend to have the same value when the bias is close to –2.0 or 2.0 V. The average conductance of K@C_{20} is about 109.939 μS, larger than that of Na@C_{20} (101.586 μS), Li@C_{20} (101.466 μS) and C_{20} (96.523 μS). So, it is safe to say that the conductance of M@C_{20} molecules increases with the doped atom from Li to K, and all the metallofullerenes have better conductibility than C_{20}.

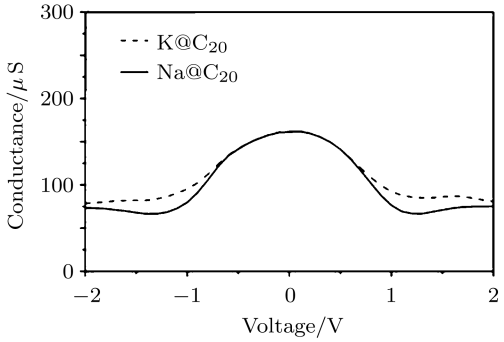


Fig. 8. The conductance–voltage (G–V) curves of both the two-probe systems.

4. Conclusions

In the present work, we have performed first-principles calculations on electronic transport properties of endohedral $M@C_{20}$(M = Na and K) metallofullerenes coupled to three-dimensional Au electrodes. Our results indicate that inserting Na or K into C_{20} fullerene obviously improves its conductibility like the case of Li atom. Under low bias voltage, the I–V curves of both $Na@C_{20}$and $K@C_{20}$ display the metal-like characteristics although nonlinear characteristic is observed under high bias. It is found that all the interstitial alkali metal atoms (Li, Na and K) can improve the conductance of C_{20} molecule. It should be noted that like $Li@C_{20,}$ $Na@C_{20}$ molecule also shows NDR behaviour, which implies that $Na@C_{20}$ could also be a candidate of NDR molecular devices. Unfortunately, this is not true for $K@C_{20}$. Obviously, alkali metal atoms can perform different effects on C_{20} molecule despite the same effect on improving its conductance, which suggests that it could design various molecular devices by inserting different alkali metal atoms into C_{20} fullerene.

References

[1] Reed M A, Zhou C, Muller C J, Burgin T P and Tour J M 1997 *Science* **278** 252

[2] Koch J, Raikh M E and Von Oppen F 2006 *Phys. Rev. Lett.* **96** 056803

[3] Zhang C, Du M H, Cheng H P, Zhang X G, Roitberg A E and Krause J L 2004 *Phys. Rev. Lett.* **92** 158301

[4] Bauschlicher Jr C W and Lawson J W 2007 *Phys. Rev.* B **75** 115406

[5] Reed M A, Chen J, Rawlett A M, Price D W and Tour J M 2001 *Appl. Phys. Lett.* **78** 3735

[6] Staykov A, Nozaki D and Yoshizawa K 2007 *J. Phys. Chem.* C **111** 1699

[7] Zhou Y H, Zheng X H, Xu Y and Zeng Z Y 2006 *J. Chem. Phys.* **125** 2447011

[8] Datta S 1995 *Electronic Transport in Mesoscopic System* (Cambridge: Cambridge University Press)

[9] Ventra M D 2008 *Electrical Transport in Nanoscale Systems* (Cambridge: Cambridge University Press)

[10] Chen J, Reed M A, Rawlett A M and Tour J M 1999 *Science* **286** 1550

[11] Esaki L 1958 *Phys. Rev.* **109** 603

[12] Sen S and Chakrabarti S 2008 *J. Phys. Chem.* C **112** 1685

[13] Gittins D I, Bethell D, Schiffrin D J and Nichols R J 2000 *Nature* **408** 67

[14] Ono T and Hirose K 2007 *Phys. Rev. Lett.* **98** 026804

[15] Noya EG, Srivastava D and Menon M 2009 *Phys. Rev.* B **79** 115432

[16] Andres R P, Bein T, Dorogi M, Feng S, Henderson J I, Kubiak C P, William M, Osifchin R G and Reifenberger R 1996 *Science* **272** 1323

[17] Kroto H W, Heath J R, O'Brien S C, Curl R F and Smalley R E 1985 *Nature* **318** 162

[18] An Y P, Yang C L, Wang M S, Ma X G and Wang D H 2009 *J. Chem. Phys.* **131** 024311

[19] Romero N A, Kim J and Martin R M 2007 *Phys. Rev.* B **76** 205405

[20] Devos A and Lannoo M 1998 *Phys. Rev.* B **58** 8236

[21] An Y P, Yang C L, Wang M S, Ma X G and Wang D H 2010 *Curr. Appl. Phys.* **10** 260

[22] Taylor J, Guo H and Wang J 2001 *Phys. Rev.* B **63** 121104

[23] Brandbyge M, Mozos J L, Ordejon P, Taylor J and Stokbro K 2002 *Phys. Rev.* B **65** 165401

[24] Soler J M, Artacho E, Gale J D, García A, Junquera J, Ordejón P and Sánchez-Portal D 2002 *J. Phys.*: *Condens. Matter* **14** 2745

[25] Taylor J, Guo H and Wang J 2001 *Phys. Rev.* B **63** 245407

[26] Xia C J, Fang C F, Hu G C, Li D M, Liu D S, Xie S J and Zhao M W 2008 *Acta Phys. Sin.* **57** 3148

[27] Chen X C, Yang J, Zhou Y H and Xu Y 2009 *Acta Phys. Sin.* **58** 3064 (in Chinese)

[28] An Y P, Yang C L, Wang M S, Ma X G and Wang D H 2010 *Acta Phys. Sin.* **59** 2010 (in Chinese)

[29] Troullier N and Martins J L 1991 *Phys. Rev.* B **43** 1993

[30] Perdew J P, Chevary J A, Vosko S H, Jackson K A, Pederson M R, Singh D J and Fiolhais C 1992 *Phys. Rev.* B **46** 6671

[31] Büttiker M, Imry Y, Landauer R and Pinhas S 1985 *Phys. Rev.* B **31** 6207

[32] Brandbyge M, Sørensen M R and Jacobsen K W 1997 *Phys. Rev.* B **56** 14956

[33] Delley B 1990 *J. Chem. Phys.* **92** 508

[34] Perdew J P and Wang Y 1992 *Phys. Ref.* B **45** 13244

[35] Yang C L, Wang M S, Sun M Y, Wang D H, Ma X G and Gong Y B 2008 *Chem. Phys. Lett.* **457** 49

[36] Sun M Y, Yang C L, Wang M S, Gong Y B, Zhu Y T and Liu W 2008 *J. Phys. Chem.* A **112** 4556

[37] Yang C L, An Y P, Sun M Y, Wang M S, Wang D H, Ma X G and Gong Y B 2009 *Chem. Phys. Lett.* **474** 311

[38] Li Y C, Yang C L, Sun M Y, Li X X, An Y P, Wang M S, Ma X G and Wang D H 2009 *J. Phys. Chem.* A **113** 1353

[39] McWhorter A L and Foyt A G 1966 *Appl. Phys. Lett.* **9** 300

[40] Brown E R, Söerström J R, Parker C D, Mahoney L J and Molvar K M 1991 *Appl. Phys. Lett.* **58** 2291